



Assessment of regional and total skeletal metabolism using ^{18}F -NaF PET/CT in patients with chronic kidney disease

Sharjeel Usmani^{1,4,8} · Najeeb Ahmed^{3,4} · Gopinath Gnanasegaran⁵ · Fahad Marafi² · Ahmed Bani-Mustafa⁶ · Tim Van den Wyngaert^{7,8}

Received: 17 February 2024 / Accepted: 8 April 2024 / Published online: 27 April 2024

© The Author(s), under exclusive licence to The Japanese Society of Nuclear Medicine 2024, corrected publication 2024

Abstract

Objective The study aims to assess regional and total bone metabolic activity in patients with chronic kidney disease using $\text{Na}[^{18}\text{F}]\text{F}$ PET and correlation between semi-quantitative indices and blood parameters.

Methods Seventy-two subjects (mean age 61.8 ± 13.8 years) were included. Of these 24/72 patients had end-stage renal disease (ESRD) ($\text{GFR} < 15 \text{ mL/min/1.73 m}^2$), 38/72 had chronic kidney disease (CKD) (GFR between 60 and $15 \text{ mL/min/1.73 m}^2$), and 10/72 were controls with normal renal function. All subjects underwent $\text{Na}[^{18}\text{F}]\text{F}$ PET-CT with a dose activity of 0.06 mCi/Kg. Regional and total skeletal metabolism were assessed with mean SUVs in a skeletal volume of interest (VOI), bone to soft tissue index (B/S), global SUV mean (GSUV mean) of the whole bone, and uptake in the femoral neck.

Results Statistically significant differences were observed in a number of ^{18}F -NaF metrics like femoral neck metabolism in CKD and ESRD groups in comparison to control in right ($P = 0.003$) and left femur ($P = 0.006$), bone to soft tissue index in the femur ($P = 0.016$) and GSUV_5 ($P = 0.006$). There is also a significant difference in SUV mean in lumbar vertebrae (L1–L4) among CKD, ESRD, and controls. There was a moderate correlation between ^{18}F -NaF PET scan uptake and blood parameters such as ALP and PTH. $\text{Na}[^{18}\text{F}]\text{F}$ uptake parameters were significantly different in low versus high bone turnover state.

Conclusions The assessment of total skeleton and regional metabolism and bone turnover in CKD patients is feasible with $\text{Na}[^{18}\text{F}]\text{F}$ PET. $\text{Na}[^{18}\text{F}]\text{F}$ can help to detect early changes in bone metabolism and assess the progression of bone disease in this complex condition. Quantification with $\text{Na}[^{18}\text{F}]\text{F}$ PET might provide better assessment of the bone turnover. The difference in $\text{Na}[^{18}\text{F}]\text{F}$ uptake in CKD compared to controls is likely related to a change in bone turnover which, however, requires further validation.

Keywords ^{18}F -NaF PET-CT · Chronic kidney disease · Metabolic bone disease · End-stage renal disease · Skeletal metabolism

✉ Sharjeel Usmani
dr_shajji@yahoo.com

¹ Department of Nuclear Medicine, Sultan Qaboos Comprehensive Cancer Care and Research Center, Muscat, Oman

² Department of Nuclear Medicine, Jaber Al-Ahmad Molecular Imaging Center, Kuwait, Kuwait

³ Department of Nuclear Medicine, Jack Brignall PET/CT Centre, Castle Hill Hospital, Cottingham, UK

⁴ Hull York Medical School, Hull, UK

⁵ Department of Nuclear Medicine, Royal Free Hospital NHS Trust, London, UK

⁶ Australian College of Kuwait, Kuwait, Kuwait

⁷ Department of Nuclear Medicine, Antwerp University Hospital, Edegem, Belgium

⁸ Faculty of Medicine and Health Sciences, University of Antwerp, Antwerp, Belgium

Introduction

Chronic kidney disease (CKD) is a global public health problem, affecting 8–16% of the population worldwide [1]. Thirty million people, or 15% of US adults, are estimated to have CKD [2]. Patients with CKD have biochemical abnormalities of calcium, phosphorus, vitamin D, and PTH; changes in bone turnover, mineralization, growth, and strength; and extraskeletal calcification. This systemic mineral metabolic syndrome is termed chronic kidney disease–mineral bone disease (CKD–MBD) and is the most common complication in patients with CKD, and is associated with high morbidity and mortality [3]. The stage of CKD at which bone disease begins to develop has not been well documented. Indeed, subclinical changes in bone metabolism can occur from much earlier stages of CKD [4], with bone abnormalities present in the majority of patients at CKD stages 3–5 and in almost all CKD patients on renal replacement therapy [5, 6].

Blood or urine-derived biomarkers can quantify bone formation and resorption, and dual-energy X-ray absorptiometry (DXA) is used to measure bone density, but difficulties remain in assessing bone metabolism in these patients due to inter- and intra-individual variability [7]. Bone turnover also has a diurnal variation influenced by food intake, blood glucose, incretin hormones, the sympathetic nervous system and osteocyte function [8]. Plasma parathormone (PTH) measurement is commonly used to evaluate CKD patients [9]. However, PTH's ability to correctly estimate bone turnover is limited, and it provides information on the overall response across the whole skeleton without providing site-specific insights [10]. Several biomarkers, such as tartrate-resistant acid phosphatase 5b (TRAP5b) and procollagen type 1 N-terminal propeptide (PINP), have been investigated, but no biomarker in clinical use has yet been proven suitable or superior to PTH to predict overall bone histology [11]. Bone biopsy is currently the reference standard for evaluating CKD patients [6], but it is invasive, costly, and gives information on only one site of the skeleton [12].

Molecular imaging modalities can quantify bone turnover non-invasively, including radiolabelled bisphosphonates scintigraphy and Na^[18F]F PET/CT. The superior pharmacokinetics of F-NaF, which is an excellent bone-seeking agent with rapid single-pass extraction by bone, makes it a promising technique to quantify bone turnover [13, 14]. Quantitative Na^[18F]F uptake reflects regional bone blood flow and osteoblastic activity, providing a functional display of regional and total skeletal metabolism [15]. The present study aims to assess the potential Na^[18F]F PET/CT imaging as a functional biomarker of regional and total skeletal metabolism in CKD patients. In addition, we wanted

to evaluate the association between semi-quantitative indices of Na^[18F]F uptake on PET/CT and serum parameters of bone metabolism.

Materials and methods

Study population

We prospectively recruited consecutive patients with chronic kidney disease or end-stage renal disease (ESRD) who were referred for Na^[18F]F PET/CT for the evaluation of skeletal metabolism with or without local or generalized bone pain. The local medical ethics committee approved the study (MOH 2019/1129). CKD was defined as structural or functional kidney abnormalities manifesting as a glomerular filtration rate (GFR) of < 60 mL/min per 1.73 m² for ≥ 3 months with or without kidney damage [16]. Patients were classified as having ESRD if the GFR was < 15 mL/min/1.73 m² or if they were on renal replacement therapy. Patients with a prior history of parathyroidectomy, pregnancy, bisphosphonate, and denosumab medication treatment in the past 6 months were excluded from the study. In addition, 10 healthy subjects (control group) matched for age, sex, and BMI without underlying kidney or bone disease underwent Na^[18F]F PET/CT for qualitative and quantitative comparison. All subjects provided informed consent for study participation.

Na^[18F]F PET/CT

All subjects were imaged on integrated PET/CT systems (Discovery 690 or 710, GE Healthcare). Images were acquired after the intravenous (IV) injection of 2.2 MBq/kg (0.06 mCi/kg) Na^[18F]F and a 60–90 min uptake period. As per institutional protocol all subjects were advised to be well hydrated and were asked to empty their urinary bladder before image acquisition. PET emission images were obtained in a three-dimensional mode at 3 min per bed position, from vertex to toes, and reconstructed with a standard iterative algorithm (ordered-subset expectation maximization, 3 iterations, and 32 subsets) and a filter cut-off of 6.4 mm as recommended by the manufacturer. A non-contrast-enhanced CT was performed using an auto-tube current of 50–120 mA determined by an automated algorithm based on the scout view to achieve a noise index of 20, 120 kVp, and pitch 1.3. The CT axial images were reconstructed in a 512 × 512 matrix, with a thickness of 2.5 mm. PET, CT, and fusion images were reviewed with Hermes Hybrid viewer version 2.2 on a PACS-integrated workstation. The scanners underwent regular quality and calibration control to meet all EARL requirements [17].

Image interpretation and quantitative analysis

Two nuclear medicine specialists, blinded to all clinical details, independently reviewed the PET/CT studies.

Mean standardized uptake value (SUV)

Attenuation-corrected PET data were normalized to injected Na[¹⁸F]F tracer activity and subject body weight to calculate the standardized uptake value (SUV). The mean SUV in the target volume of interest (VOI) is calculated as:

$$\text{SUV}_{\text{mean}} = \frac{\text{mean activity concentration (Bq/ml)} \times \text{body weight (gm)}}{\text{injected activity (Bq)}}$$

Regional bone metabolism

To quantify regional bone metabolism, the target bone VOI was a sphere with a diameter of 2 cm (volume 4.2 cm³) centered on the L1–L4 vertebrae. Other target bone VOIs were the left parietal skull bone and the neck of the left femur. Background spherical VOIs of the same diameter were centered on the right or left psoas muscle at the L3 level, the aorta, and subcutaneous fat tissue (Supplementary Figure S1A).

Bone to soft tissue (BTS) index analysis

The bone to soft tissue index was calculated by dividing the SUV_{mean} of bone by the SUV_{mean} of soft tissue. The target bone VOI was a sphere with a diameter of 2 cm (volume 4.2 cm³) centered over the proximal diaphysis of the right femur below the intertrochanteric region. A background soft tissue VOI sphere with the same diameter was centered on the upper medial thigh region (Supplementary Figure S1A). Another bone to soft tissue index was calculated over the skull and brain parenchyma (skull/brain).

Total uptake of Na[¹⁸F]F in the femoral neck

The ¹⁸F-NaF uptake in the neck region was segmented using CT scan landmarks. The inner boundary of the neck region was defined by the epiphyseal line that was identifiable on CT. The outer boundary of the neck was defined by the intertrochanteric ridge (Supplementary Figure S1B) [18, 19].

Total uptake of Na[¹⁸F]F in the skeleton (GSUV_{mean})

The global SUV mean was measured in the whole axial skeleton of each patient. Whole bone measurements

included the axial and proximal appendicular skeleton, excluding the skull, jaw, and appendages more than 20 cm distal to the glenohumeral joint and more than 10 cm inferior to the lowest portion of the ischium (Supplementary Figure S1C). After manual exclusions were made to define a VOI, a region-growing algorithm with a lower threshold of 150 Hounsfield units (HU), followed by morphological closing, was applied to the CT image, segmenting only the bony skeleton. The global mean SUV (GSUV_{mean}) was calculated as the average of the SUVs of all voxels within the VOI [20]. The GSUV_{mean} was calculated with two threshold values of SUV 2 and SUV 5 (GSUV₂ and GSUV₅).

Laboratory assessments

The renal function of the patients was assessed by serum urea, creatinine, and eGFR. Serum-ionized calcium, phosphorus, bone-specific alkaline phosphatase (bALP), total vitamin D, and parathormone (PTH) were performed in all patients. The intact PTH (iPTH) level was measured by a double-antibody chemiluminescence immunoassay ± 15 days from the Na[¹⁸F]F PET/CT study. Patients were classified as having a high bone turnover state using the PTH cut-off value of 7.2 pmol/L.

Statistical analysis

Statistical analysis was performed using the statistical package for the social sciences (SPSS 12.0, Chicago, IL, USA). Results were presented as the mean ± standard deviation (SD). Correlations between blood profile parameters and fluoride activity on PET were assessed using Pearson correlation and interpreted as follows: 0.0–0.2 = very weak, 0.2–0.4 = weak, 0.4–0.6 = moderate, 0.6–0.8 = strong, 0.8–1.0 very strong association [21]. For estimating the difference between the means of Na[¹⁸F]F in different groups, we used a one-way analysis of variance (ANOVA) after logarithmic transformation. Pairwise comparisons in the groups are made using Tukey pairwise post hoc testing to determine whether there is a difference between the mean of all possible pairs using a studentized range distribution. Optimal cut-points for continuous predictors of ¹⁸F-NaF parameters to discriminate high bone turnover were determined with receiver operating characteristics (ROC) curves, where the sensitivity and specificity of the test are equal; the point on the curve with minimum distance from the left-upper corner of the unit square. AUC values were interpreted as previously published [22]. *P* values less than 0.05 were considered to be significant.

Results

Study population

In addition to 10 control subjects, sixty-two patients fulfilled the inclusion criteria and were enrolled. In total, 31 males and 41 females were analyzed, with a mean age of 61.9 ± 13.8 (26–84) years. 38 patients were classified as having CKD (20 males, 18 females; mean age 64.6 ± 10.8 [41–84] years) and 24 as ESRD (7 males, 17 females; mean age 55.9 ± 17.2 [26–84] years). The control group consisted of 4 men and 6 women (mean age 65.3 ± 11.5 [52–82] years). Additional patient characteristics are presented in Table 1.

Quantification of Na^{[18F]F} uptake

Na^{[18F]F} PET/CT images showed high tracer extraction with negligible soft tissue background uptake in all patients: psoas muscle (SUVmean 1.20 ± 0.40), aorta (SUVmean 1.67 ± 0.69), and subcutaneous fat tissue (SUVmean 0.50 ± 0.88). Differences in quantitative ¹⁸F-NaF PET/CT indices between controls and patients are summarized in Supplementary Table S1.

Comparison between control, CKD, and ESRD groups

The mean SUVs measured at the L1–L3 vertebrae were significantly higher in ESRD patients (all $P < 0.01$) than in CKD patients (Supplementary Figure S2A–C). Only the uptake of ¹⁸F-NaF in L4 was significantly higher in ESRD patients (11.9 ± 4.77) compared to CKD patients

(8.41 ± 2.30 ; $P < 0.001$) and controls (8.78 ± 1.55 ; $P = 0.032$) (Supplementary Figure S2D). The SUV mean in the femoral neck of both femurs was significantly higher in ESRD patients compared to CKD patients and controls (all $P < 0.05$). There were no significant differences in mean femur SUVs between CKD patients and controls (Supplementary Figure S3A–B). The femoral bone to soft tissue index was significantly different between CKD and ESRD patients and control subjects ($P = 0.016$), with a higher mean value in ESRD patients (4.6 ± 2.48) compared to controls (2.55 ± 0.53 ; $P = 0.014$). No other statistically significant differences existed between groups, nor for the skull to soft tissue index ($P = 0.328$) (Supplementary Figure S3C–D).

The total SUV mean (GSUV₅) showed overall differences between groups ($P = 0.006$), driven by a higher uptake in controls (8.7 ± 0.65) compared to CKD patients (7.7 ± 0.86 ; $P = 0.009$). A small difference in mean GSUV₂ was observed between CKD patients (4.58 ± 0.57) and ESRD patients (5.06 ± 0.91 ; $P = 0.024$) (Supplementary Figure S3E–F). Details of all metrics and pairwise comparisons are provided in Supplementary Table S2 and Supplementary Table S3.

Comparison of low/normal versus high bone turnover patients

In our study, 72.5% of patients ($n = 45$, CKD:ESRD: 24:21) had a hyperparathyroid (high turnover) state, while 27.5% ($n = 17$, CKD:ESRD: 14:3) had an adynamic (low/normal turnover) state based on PTH levels. When analyzing the Na^{[18F]F} uptake parameters according to turnover state, significant differences existed between both groups for all indices (Table 2). The mean SUVs measured at the

Table 1 Baseline patient characteristics of study subjects

	Mean \pm SD		
	Control ($N = 10$)	CKD ($N = 38$)	ESRD ($N = 24$)
Age (years)	65.3 ± 11.5	64.6 ± 10.8	55.9 ± 17.2
Injected activity (mCi)	4.54 ± 0.96	4.87 ± 1.0	4.39 ± 0.82
Effective dose of ¹⁸ F-NaF (mSv)	4.0 ± 0.85	4.32 ± 0.91	3.9 ± 0.72
Female:Male	6:4	18:20	17:7
BMI (kg/m ²)	31.3 ± 11.7	30.5 ± 7.3	29.42 ± 5.63
eGFR	91.0 ± 12.0	43.0 ± 9.6	11.4 ± 2.96
Serum calcium (reference 2.1–2.55 mmol/L)	2.25 ± 0.15	2.12 ± 0.24	1.95 ± 0.39
Phosphorus (reference 0.74–1.52 mmol/L)	1.07 ± 0.12	1.27 ± 0.44	1.91 ± 0.37
ALP (reference 40–150 U/L)	99.9 ± 42.4	221.5 ± 220.2	242.9 ± 172.1
iPTH (reference 1.1–7.2 pmol/L)	7.0 ± 1.8	36.96 ± 48.73	81.25 ± 66.68
Vitamin D (reference > 75 nmol/L)	78.81 ± 15.09	64.33 ± 13.65	62.89 ± 18.15

Table 2 Quantitative parameters of ^{18}F -NaF PET-CT in patients with low/normal and high bone turnover

Quantitative parameter	<i>N</i> = 17 Low/normal turnover /adynamic bone disease	<i>N</i> = 45 High turnover /hyperparathyroid bone disease	Overall <i>P</i> value
Global skeletal uptake			
Global mean SUV ₅ (GSUVmean)	7.28 ± 0.63	8.20 ± 1.04	0.001
Global mean SUV ₂ (GSUVmean)	4.17 ± 0.40	4.99 ± 0.73	< 0.001
Bone to soft tissue index			
Femur/thigh	2.79 ± 1.10	4.65 ± 2.19	0.001
Skull/brain	9.55 ± 5.94	18.2 ± 15.23	0.026
Regional bone metabolism			
Right femoral neck	3.78 ± 0.90	6.41 ± 2.15	< 0.001
Left femoral neck	3.92 ± 0.96	6.76 ± 2.31	< 0.001
L1	7.83 ± 1.57	11.0 ± 3.73	0.001
L2	7.53 ± 1.17	10.53 ± 3.50	0.001
L3	7.42 ± 1.18	10.61 ± 4.58	0.006
L4	7.31 ± 1.52	10.65 ± 4.06	0.003

ANOVA test. The significance level is 0.05

*SUV*₅ threshold SUV = 5, *SUV*₂ threshold SUV = 2

L1–L4 vertebrae were higher in the high turnover group compared to the low/normal turnover group (all $P < 0.006$) (Fig. 1A–D). The mean uptake in the femoral neck of both femurs was approximately 1.7 times higher in patients with a high bone turnover state (all $P < 0.001$) (Fig. 2A, B). Similarly, the bone to soft tissue indices were approximately 1.5–2.0-fold higher in patients with high bone turnover states (all $P < 0.05$) (Fig. 2C, D). The global SUV mean (GSUV₅ and GSUV₂) were between 13 and 20% higher in patients with high bone turnover (all $P < 0.001$) (Fig. 2E, F).

Using ROC curve analysis, excellent AUC values (> 0.80) were observed for SUV mean in the femurs (AUC > 0.87), the femur/thigh ratio (AUC 0.84), and the GSUV₂ (AUC 0.85) to discriminate low/normal from high bone turnover states (Table 3). The highest AUC values were observed for the left femur, the L2 vertebra, and the femur BTS and GSUV indices (Supplementary Figure S4).

Correlation with laboratory assessments

Strong positive correlations between the mean SUV of Na[^{18}F]F in the L2–L4 vertebrae and both femurs were consistently observed with serum bALP and PTH levels (all $P < 0.01$) (Table 4). Similarly, the measures of global skeletal Na[^{18}F]F uptake GSUV₅ and GSUV₂ showed moderate to strong positive correlations with bALP and PTH (all $P < 0.001$). In contrast, only weak correlations were observed between the bone to soft tissue ratios and bALP and PTH, even though these were statistically significant (all $P < 0.05$). Weak negative correlations also existed between the various Na[^{18}F]F uptake indices and serum vitamin D

and ionized calcium levels, but only with some being statistically significant. Finally, weak to moderate positive correlation was observed between serum phosphorus and the mean SUV of Na[^{18}F]F in the global skeleton and in the vertebrae and femurs (all $P < 0.05$), but not for the bone to soft tissue ratios. Other correlation coefficients are listed in Table 4.

Qualitative imaging findings

In addition to the quantitative analysis, the following qualitative clinical findings were documented in the patient cohort: osteitis fibrosa cystica (brown tumor) ($n = 5$), avascular necrosis ($n = 1$), vertebral collapse ($n = 2$), sacral insufficiency fracture ($n = 2$), and destructive osteoarthropathies and spondyloarthropathy ($n = 3$) (Supplementary Figure S5).

Discussion

CKD produces changes in bone metabolism that affect bone structure and turnover, yet assessing bone metabolism remains difficult. Radionuclide imaging methods have been used in the past to provide a better understanding of bone metabolism in CKD patients. For example, quantitative bone scintigraphy with [$^{99\text{m}}\text{Tc}$]Tc-MDP using a bone to soft tissue ratio was found to be able to evaluate bone metabolism in hemodialysis patients, but technical limitations in tracer quantification hampers this technique [23, 24]. In contrast, Na[^{18}F]F PET/CT has superior imaging and quantification properties, potentially making it a useful complementary

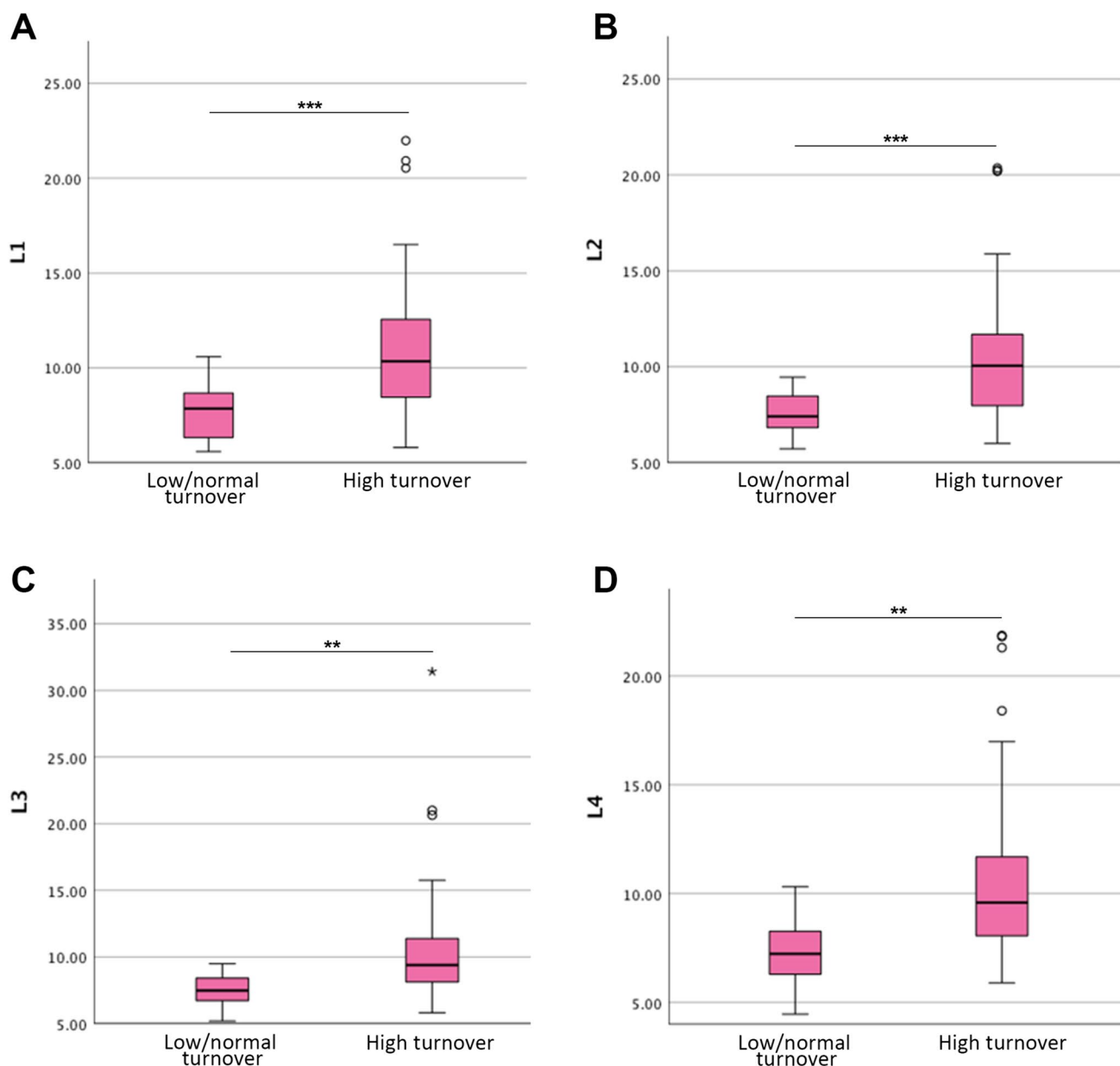


Fig. 1 Box plots of mean SUVs measured in skeletal volumes of interest (VOI) in the lumbar spine L1–L4 in patients with low/normal and high bone turnover. Significant differences are flagged using hori-

zontal lines and asterisks (* $P < 0.05$; ** $P < 0.01$; *** $P < 0.001$). The outliers are plotted as a small circle and a star on the box-plot

tool for examining changes in regional and total bone metabolism in CKD patients [25].

Quantitative imaging using Na[^{18}F]F PET/CT assesses bone metabolism and quantifies bone turnover, reflecting regional bone blood flow and osteoblastic activity [26]. There are two primary methods of quantification; the first is dynamic kinetic modeling (Hawkins method) using bone plasma clearance [27], which is the most accurate and provides an absolute measurement of tracer activity and kinetics [28]. However, it requires sequential arterial blood sampling and activity measurement in addition to long image

acquisition times, making the method cumbersome and unattractive for routine clinical use. For example, a study by Aaltonen L et al. reported that the net influx rate (K_i) of Na[^{18}F]F in bone could work as a noninvasive diagnostic tool using a 1-h-long PET/CT dynamic scan to confirm high turnover/hyperparathyroid bone disease before parathyroidectomy or to rule out low/normal turnover/adynamic bone disease before initiating antiresorptive medication [29]. Recently a simplified protocol was used to calculate K_i at multiple sites in the skeleton without loss of accuracy or precision that required 2–3 venous blood samples and a 4-min

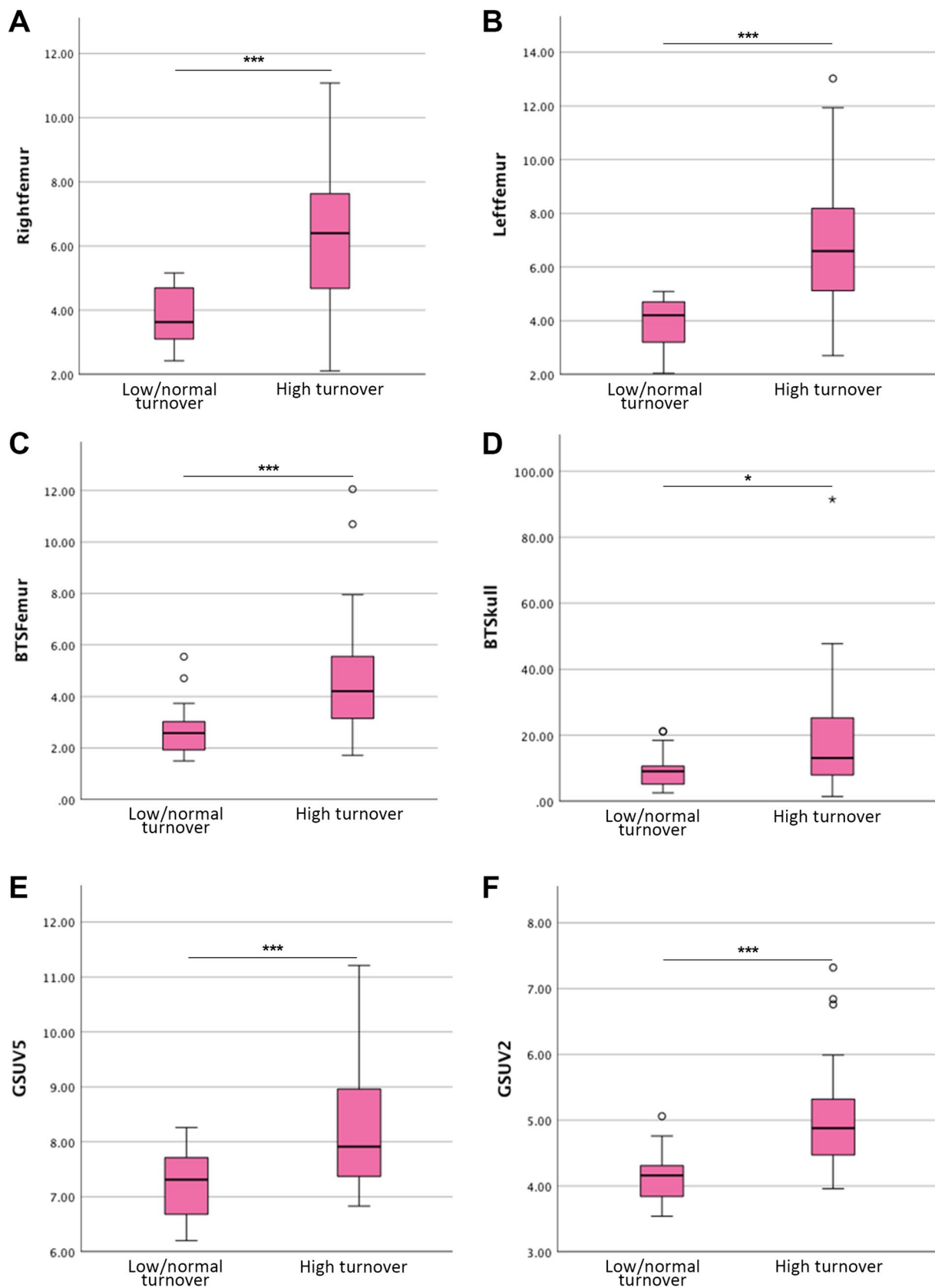


Fig. 2 Box plots of total femoral uptake, BTS femur, BTS skull, GSUV in patients with low/normal and high bone turnover. Significant differences are flagged using horizontal lines and asterisks (* $P < 0.05$; ** $P < 0.01$; *** $P < 0.001$). The outliers are plotted as a small circle and a star on the box-plot

Table 3 The ROC curve analysis defining the optimal cut-off point for ^{18}F -NaF indices to discriminate low/normal and high bone turnover

Quantitative parameter	AUC (95% CI)	Optimal cut-off value	Sensitivity (%)	Specificity (%)
BTS femur	0.836 (0.716–0.956)	3.03	78.6	80.0
BTS skull	0.697 (0.547–0.847)	10.7	66.7	73.3
GSUV ₅	0.735 (0.597–0.872)	8.31	38.1	100.0
GSUV ₂	0.854 (0.746–0.962)	4.34	85.7	73.3
R. femur	0.869 (0.774–0.964)	5.4	61.9	100.0
L. femur	0.902 (0.826–0.979)	5.1	76.2	100.0
L1	0.783 (0.658–0.909)	8.73	71.4	80.0
L2	0.816 (0.706–0.926)	9.52	54.8	100.0
L3	0.799 (0.683–0.915)	8.01	76.2	73.3
L4	0.804 (0.683–0.925)	8.32	71.4	80.0

Table 4 Pearson's correlations between ^{18}F -NaF PET indices and blood parameters

Quantitative parameter	Blood parameters					
	bALP	iPTH	Vit. D	Calcium	Phosphorus	eGFR
BTS femur	0.344**	0.338**	−0.217*	0.004	0.169	−0.186
BTS skull	0.384**	0.267*	−0.022	0.226	0.203	−0.117
GSUV ₅	0.608***	0.645***	−0.229	0.029	0.305*	−0.213
GSUV ₂	0.535***	0.626***	−0.282*	0.033	0.292*	−0.290
R. femur	0.680***	0.698***	−0.227	−0.289*	0.449***	−0.309*
L. femur	0.724**	0.746**	−0.234	−0.190	0.391**	−0.278*
L1	0.602**	0.581*	−0.242	−0.116	0.383**	−0.303*
L2	0.614***	0.614**	−0.289*	−0.104	0.436***	−0.383**
L3	0.607***	0.654***	−0.297*	−0.079	0.471***	−0.356**
L4	0.630***	0.671***	−0.282*	−0.128	0.549***	−0.434***

SUV₅ threshold SUV = 5, SUV₂ threshold SUV = 2

* is significant at the 0.05 level, ** is significant at the 0.01 level, and *** is significant at the 0.001 level

or 12-min PET scan to measure Ki values, without the need for a 60-min dynamic scanning [30].

The second method measures the standard uptake values (SUVs), which is the mean $\text{Na}[^{18}\text{F}]\text{F}$ concentration in the bone for an injected activity normalized by body weight [31]. A static SUV measurement in the tissue region of interest is an easy and simple method requiring no additional venous sampling and only a short static acquisition, making it a more suitable approach for clinical implementation [32]. Indeed, in a prior proof-of-concept study of $\text{Na}[^{18}\text{F}]\text{F}$ PET/CT in ESRD patients on dialysis, we demonstrated the high extraction of $\text{Na}[^{18}\text{F}]\text{F}$ and that using static SUV measurements to calculate the bone to soft tissue uptake could discriminate ESRD patients from controls (4.03 versus 2.48; $P=0.01$) [33]. The two measurements SUV and Ki remain well correlated in most circumstances. SUV is expected to have the smallest error in calculation because the measurement involves evaluating only bone uptake and avoids the additional sources of error from measuring the arterial

input function. Ki is more accurate than SUV particularly in some circumstances for example measuring response to treatment when studying drugs that have a potent effect on bone remodeling across the whole skeleton [34].

In the current study, we also provide evidence that the static $\text{Na}[^{18}\text{F}]\text{F}$ semi-quantitative parameters based on SUV significantly differ between patients with different stages of CKD. Overall, control subjects had the lowest regional $\text{Na}[^{18}\text{F}]\text{F}$ uptake and patients with ESRD the highest uptake, with an average of 1.4-fold increase in absolute value, but with considerable overlap and with CKD patient in between. In contrast, global uptake parameters (GSUV) were lowest in CKD patients, compared to controls and ESRD patients. The $\text{Na}[^{18}\text{F}]\text{F}$ uptake metrics (i.e., SUV of the femur or vertebra, BTS and GSUV) could also discriminate the low/normal and high turnover states in renal osteodystrophy with high AUC values using the identified cut-offs (Table 3). Here, high-turnover patients had consistently higher absolute values of $\text{Na}[^{18}\text{F}]\text{F}$ uptake across all studied regional and global

uptake parameters. BTS values were approximately 1.5–2.0-fold higher in patients with high bone turnover (all $P < 0.05$), providing better separation of the populations.

Across the different regional measurements examined in this study, the uptake at the femoral neck emerged as a consistent discriminator between the different populations of CKD and ESRD, and of low/normal and high turnover states with excellent AUCs. In addition, the femoral neck is not affected by osteoarthritic changes that can cause increased Na^{18}F uptake, in contrast to the spine. In a recent study by Rhodes et al., the uptake of Na^{18}F in the femoral neck was also found to correlate well with bone mineral density (BMD), with the potential to provide additional information when assessing hip fracture risk [35]. Based on these results, we propose the femoral neck as the optimal site for assessing regional bone turnover in patients with CKD–MBD.

In the current study, we also investigated measures of overall skeletal metabolism (GSUV) to evaluate systemic osseous metabolism more accurately, representing a novel approach compared to prior Na^{18}F PET/CT studies in CKD–MBD. While the global SUV_{mean} (GSUV_s), as measured by CT segmentation of the entire axial skeleton and proximal appendicular skeleton, showed significantly higher values in controls compared to CKD patients, considerable overlap between CKD and ESRD patients exists, limiting its usefulness. The GSUV has different results for group differences depending on the threshold settings. We, therefore, used two GSUV thresholds: SUV 2 (GSUV₂) and SUV 5 (GSUV₅) for analysis to address this potential inconsistency in the GSUV on different threshold settings. However, it is important to emphasize that due to these limitations interpretation of this specific metric requires caution. In contrast,

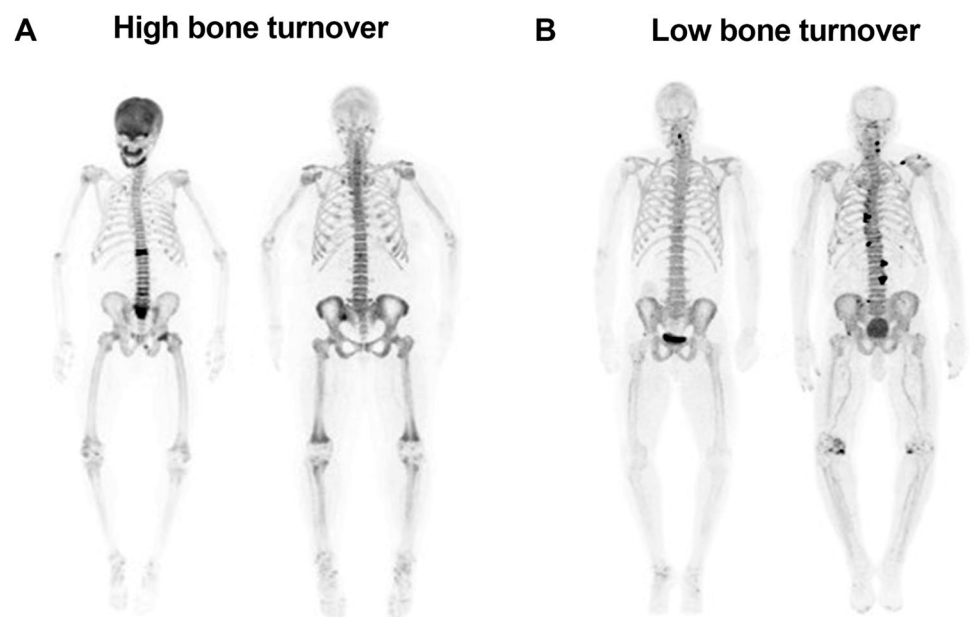
a good separation and AUC value was observed for GSUV measurements to distinguish low/normal and high turnover states, with higher values in patients with high turnover.

Our study is the first to evaluate Na^{18}F PET/CT in CKD patients using a global assessment approach that may be more pertinent to patients with generalized bone disorders. A major advantage of GSUV is that it can be calculated using a semiautomated method, reducing operator variability and possibly improving the poor reproducibility of PET quantification [36]. Nevertheless, care should be taken to manually exclude age-related metabolically active osteoarthritic changes in the spine before the analysis and further study is needed to improve this process.

In pioneering work with dynamic Na^{18}F PET imaging, Messa et al. demonstrated a close relationship between the bone influx rate of Na^{18}F and serum alkaline phosphatase and PTH values in patients with renal osteodystrophy and primary hyperparathyroidism [37]. Our study showed strong correlations between the more convenient static SUV measures (GSUV_s, GSUV₂, and SUV_{mean} of the femoral neck and L1–L4 vertebrae) and bone turnover markers, including ALP and PTH. While we did not assess bone histomorphology, other researchers have demonstrated correlations between Na^{18}F uptake and histomorphometric parameters, such as bone formation rate, activation frequency, and osteoclast and osteoblast surfaces and mineralized surfaces in dialysis patients. Interestingly, Na^{18}F PET/CT was superior to PTH in differentiating low/normal turnover from non-low turnover with high AUC (0.82) [38].

High bone turnover appears as a diffuse increase in tracer uptake on Na^{18}F PET/CT in the axial and appendicular skeleton (Fig. 3). Additionally, the calvarium can

Fig. 3 **A** High bone turnover: Na^{18}F MIP image demonstrates diffuse increased activity within the axial and proximal appendicular skeleton. No tracer activity is seen in the kidneys and the urinary bladder. Quantitative analysis of ^{18}F -NaF shows high total and regional bone metabolism. **B** Low bone turnover: Na^{18}F MIP image shows relatively low tracer uptake with low total and regional bone metabolism on quantitative analysis



be thickened and show increased osteoblastic activity, or a “rose bead pattern” of uptake at the costochondral junction or increased uptake near the vertebral endplates (“Rugger jersey sign”) can be seen. There may be lack of kidney and bladder activity [39]. In our study population, hyperparathyroidism manifesting as osteitis fibrosa cystica (brown tumor) was seen in 5 patients. Typically, Na¹⁸F]F PET/CT is useful for detecting osteitis fibrosa cystica and brown tumors by showing either increased osteoblast activity or high vascularization in the lesions [40, 41].

The limitations of our study are the relatively small number of patients and lack of a true reference standard. The global uptake in the femoral neck was completed semi-automatically by drawing VOI around the femoral neck, which is not as ideal as automatic segmentations can be less time-consuming. The VOIs were drawn manually and subjected to human error. Future studies could use more sophisticated artificial intelligence (AI) bone segmentation algorithms to investigate simple thresholding and reduce the time penalty of this analysis. Our study used conventional SUVs normalized to body weight. However, as Na¹⁸F]F uptake is primarily in the skeleton, it should be investigated if normalizing SUVs for the skeletal volume instead of the body weight would be better. SUV measurements can be affected by competing uptake in the kidneys, bone lesions and tracer availability, this competition may differ substantially from patient to patient due to variations in the whole-body metabolism of the tracer. Other confounding artefacts of SUV measurements include atherosclerosis, vascular calcification, arthritis and inflammation. Another limitation includes considering PTH as a biomarker of bone turnover. In CKD patients, PTH levels are not always a good predictor of bone turnover, and current PTH assays have various methodological limitations [42]. The impact of concomitant medication could also not be assessed, except for those excluded in the study participation criteria. Further studies are needed to assess the overall clinical utility of this technique, for example, the potential impact on the management of bone and mineral disorders. There is a potential gender imbalance in the ESRD group with more females (17 females, 7 males). This could introduce bias if there are gender-specific differences in bone metabolism or Na¹⁸F]F biodistribution.

Conclusions

Our study demonstrates the feasibility of assessing global and regional skeletal bone turnover in CKD-MBD patients using SUV measures derived from static Na¹⁸F]F PET/CT acquisitions, coupled with novel CT segmentation techniques. This approach offers a clinically significant simplification compared to dynamic methods. Our findings underscore the complementary role of Na¹⁸F]F PET as a

noninvasive semi-quantitative diagnostic imaging biomarker for evaluating bone metabolism in patients with metabolic conditions, leading to high or low bone turnover including those with CKD. While our study provides valuable insights, further research is necessary to fully understand the potential clinical implications of this technique in the management of CKD. Future investigations should focus on determining its precise role and integration into clinical practice, thus ensuring its utility in improving patient outcomes and informing treatment decisions.

Supplementary Information The online version contains supplementary material available at <https://doi.org/10.1007/s12149-024-01929-1>.

Data availability The data of this study can be available on request from the corresponding author.

Declarations

Conflict of interest The authors declare that they have no conflict of interest. No financial help or grant is taken by any governmental and non-governmental organization.

Ethical approval All procedure performed in studies involving human participants were in accordance with the ethical standard of the institutional and/or national research committee and with the 1964 Helsinki Declaration and its later amendments or comparable ethical standards.

Informed consent The institutional review board of our institute approved this study and all subjects provided informed consent for study participation.

References

1. Jha V, Gaecia-Garcia G, Iseki K, et al. Chronic kidney disease: global dimension and perspectives. *Lancet*. 2013;382:260–72.
2. National Institutes of Health. 2016 USRDS Annual Data Report: Epidemiology of Kidney Disease in the United States. Bethesda, MD: National Institutes of Health, National Institute of Diabetes and Digestive and Kidney Diseases; 2016.
3. Ketteler M, Block GA, Evenepoel P, et al. KDIGO 2017 clinical practice guideline update for the diagnosis, evaluation, prevention, and treatment of CKD-MBD. *Kidney Int Suppl*. 2017;7(Suppl 1):1–59.
4. Coen G, Ballanti P, Bonucci E, et al. Renal osteodystrophy in predialysis and hemodialysis patients: comparison of histologic patterns and diagnostic predictivity of intact PTH. *Nephron*. 2002;91:103–11.
5. Fukagawa M, Hamada Y, Nakanishi S, et al. The kidney and bone metabolism: a nephrologist’s view. *J Bone Miner Metab*. 2006;24:434–8.
6. National Kidney Foundation. K/DOQI clinical practice guidelines for bone metabolism and disease in chronic kidney disease. *Am J Kidney Dis*. 2003;42(suppl 3):S1–201.
7. Green AD, Colon-Emeric CS, Bastian L, et al. Does this woman have osteoporosis? *JAMA*. 2004;292:2890–900.
8. Hygum K, Starup-Linde J, Harsløf T, et al. The diurnal variation of bone formation is attenuated in adult patients with type 2 diabetes. *Eur J Endocrinol*. 2019;181:221–31.
9. Lehmann G, Stein G, Hüller M, et al. Specific measurement of PTH (1–84) in various forms of renal osteodystrophy

- (ROD) as assessed by bone histomorphometry. *Kidney Int.* 2005;68:1206–14.
10. Sprague SM, Bellorin-Font E, Jorgetti V, et al. Diagnostic accuracy of bone turnover markers and bone histology in patients with CKD treated by dialysis. *Am J Kidney Dis.* 2016;67:559–66.
 11. Salam S, Gallagher O, Gossiel F, Paggiosi M, Khwaja A, Eastell R. Diagnostic accuracy of biomarkers and imaging for bone turnover in renal osteodystrophy. *J Am Soc Nephrol.* 2018;29:1557–65.
 12. Evenepoel P, Behets GJS, Laurent MR, D’Haese PC. Update on the role of bone biopsy in the management of patients with CKD-MBD. *J Nephrol.* 2017;30:645–52.
 13. Czernin J, Satyamurthy N, Schiepers C. Molecular mechanisms of bone ^{18}F -NaF deposition. *J Nucl Med.* 2010;51:1826–9.
 14. Grant FD, Fahey FH, Packard AB, et al. Skeletal PET with ^{18}F -fluoride: applying new technology to an old tracer. *J Nucl Med.* 2008;49:68–78.
 15. Raynor W, Houshmand S, Gholami S, et al. Evolving role of molecular imaging with (^{18}F) -sodium fluoride PET as a biomarker for calcium metabolism. *Curr Osteoporos Rep.* 2016;14:115–25.
 16. Kidney Disease: Improving Global Outcomes (KDIGO) CKD-MBD Working Group. KDIGO clinical practice guideline for the diagnosis, evaluation, prevention, and treatment of chronic kidney disease—mineral and bone disorder (CKD–MBD). *Kidney Int.* 2009;76(Suppl 113):S1–130.
 17. Lasnon C, Salomon T, Desmots C, Dô P, Oulkhoudir Y, Madelaine J, et al. Generating harmonized SUV within the EANM EARL accreditation program: software approach versus EARL-compliant reconstruction. *Ann Nucl Med.* 2017;31:125–34.
 18. Raynor W, Ayubcha C, Shamchi SP, Zadeh MZ, Emamzadehfard S, Werner T, et al. Assessing global uptake of ^{18}F -sodium fluoride in the femoral neck: a novel quantitative technique to evaluate changes in bone turnover with age. *J Nucl Med.* 2017;58:1223.
 19. Raynor W, Houshmand S, Gholami S, Werner T, Alavi A. Assessment of bone turnover by measuring global uptake of ^{18}F -sodium fluoride in the femoral neck, a novel method for early detection of osteoporosis. *J Nucl Med.* 2016;57:1769.
 20. Zirakchian Zadeh M, Østergaard B, Raynor WY, et al. Comparison of ^{18}F -sodium fluoride uptake in the whole bone, pelvis, and femoral neck of multiple myeloma patients before and after high-dose therapy and conventional-dose chemotherapy. *Eur J Nucl Med Mol Imaging.* 2020;47:2846–55.
 21. Evans JD. Straightforward statistics for the behavioral sciences. Thomson Brooks/Cole Publishing Co; 1996.
 22. Hosmer DW, Lemeshow S. Applied logistic regression. 2nd ed. New York, NY: Wiley; 2000. p. 160–4.
 23. Kurata S, Ishibashi M, Nishida H, Hiromatsu Y, Hayabuchi N. A clinical assessment of the relationship between bone scintigraphy and serum biochemical markers in hemodialysis patients. *Ann Nucl Med.* 2004;18:513–8.
 24. Nishida H, Kaida H, Ishibashi M, et al. Usefulness of bone uptake ratio of bone scintigraphy in hemodialysis patients. *Ann Nucl Med.* 2005;19:91–4.
 25. Frost ML, Blake GM, Park-Holohan SJ, et al. Long-term precision of ^{18}F -fluoride PET skeletal kinetic studies in the assessment of bone metabolism. *J Nucl Med.* 2008;49:700–7.
 26. Jadvar H, Desai B, Conti PS. Sodium ^{18}F -fluoride PET/CT of bone, joint, and other disorders. *Semin Nucl Med.* 2015;45:58–65.
 27. Hawkins RA, Choi Y, Huang SC, et al. Evaluation of the skeletal kinetics of fluorine-18-fluoride ion with PET. *J Nucl Med.* 1992;33:633–42.
 28. Frost ML, Cook GJR, Blake GM, et al. A prospective study of risedronate on regional bone metabolism and blood flow at the lumbar spine measured by ^{18}F fluoride positron emission tomography. *J Bone Miner Res.* 2003;18:2215–22.
 29. Aaltonen L, Koivuvuitta N, Seppänen M, et al. Bone histomorphometry and ^{18}F -sodium fluoride positron emission tomography imaging: comparison between only bone turnover-based and unified TMV-based classification of renal osteodystrophy. *Calcif Tissue Int.* 2021;109:605–14.
 30. Puri T, Frost ML, Moore AEB, et al. Utility of a simplified $[^{18}\text{F}]$ sodium fluoride PET imaging method to quantify bone metabolic flux for a wide range of clinical applications. *Front Endocrinol (Lausanne).* 2023;14:1236881.
 31. Uchida K, Nakajima H, Miyazaki T, et al. Effects of alendronate on bone metabolism in glucocorticoid-induced osteoporosis measured by ^{18}F -fluoride PET: a prospective study. *J Nucl Med.* 2009;50:1808–14.
 32. Siddique M, Frost ML, Blake GM, et al. The precision and sensitivity of (^{18}F) -fluoride PET for measuring regional bone metabolism: a comparison of quantification methods. *J Nucl Med.* 2011;52:1748–55.
 33. Usmani S, Marafi F, Esmail A, et al. A proof of concept study analyzing the clinical utility of ^{18}F -sodium fluoride (NaF) PET-CT in skeletal staging of oncology patients with end-stage renal disease on dialysis. *Nucl Med Commun.* 2017;38:1067–75.
 34. Assiri R, Knapp K, Fulford J, Chen J. Correlation of the quantitative methods for the measurement of bone uptake and plasma clearance of ^{18}F -NaF using positron emission tomography: systematic review and meta-analysis. *Eur J Radiol.* 2022;146:110081.
 35. Rhodes S, Batzdorf A, Sorci O, et al. Assessment of femoral neck bone metabolism using ^{18}F -sodium fluoride PET/CT imaging. *Bone.* 2020;136:115351.
 36. Zadeh MZ, Raynor WY, Seraj SM, et al. Evolving roles of fluoro-deoxyglucose and sodium fluoride in assessment of multiple myeloma patients: introducing a novel method of PET quantification to overcome shortcomings of the existing approaches. *PET Clin.* 2019;14:341–52.
 37. Messa C, Goodman WG, Hoh CK, et al. Bone metabolic activity measured with positron emission tomography and $[^{18}\text{F}]$ fluoride ion in renal osteodystrophy: correlation with bone histomorphometry. *J Clin Endocrinol Metab.* 1993;77:949–55.
 38. Aaltonen L, Koivuvuitta N, Seppänen M, et al. Correlation between ^{18}F -sodium fluoride positron emission tomography and bone histomorphometry in dialysis patients. *Bone.* 2020;134:115267.
 39. Usmani S, Ahmed N, Gnanasegaran G, Marafi F, van den Wyngaert T. Update on imaging in chronic kidney disease-mineral and bone disorder: promising role of functional imaging. *Skelet Radiol.* 2022;51:905–22.
 40. Deng Y, Shen X, Lei L, Zhang W. Osteitis fibrosa cystica caused by hyperparathyroidism shown on ^{18}F -NaF PET/CT. *Clin Nucl Med.* 2020;45:577–9.
 41. Graf C, Huellner M, Tschopp O, Bode-Lesniewska B, Schmid C. (^{18}F) -NaF-PET/CT in patients with primary hyperparathyroidism and brown tumors. *J Bone Miner Metab.* 2020;38:299–309.
 42. Pontoriero G, Cozzolino M, Locatelli F, Brancaccio D. CKD patients: the dilemma of serum PTH levels. *Nephron Clin Pract.* 2010;116:c263–8.

Publisher's Note Springer Nature remains neutral with regard to jurisdictional claims in published maps and institutional affiliations.

Springer Nature or its licensor (e.g. a society or other partner) holds exclusive rights to this article under a publishing agreement with the author(s) or other rightsholder(s); author self-archiving of the accepted manuscript version of this article is solely governed by the terms of such publishing agreement and applicable law.